

Cross-reality Location Privacy Protection in 6G-enabled Vehicular Metaverses: An LLM-enhanced Hybrid Generative Diffusion Model-based Approach

Xiaofeng Luo¹, Jiayi He¹, Jiawen Kang^{1*}, Ruichen Zhang², Zhaoshui He¹,
Ekram Hossain³ & Dong In Kim⁴

¹*School of Automation, Guangdong University of Technology, Guangzhou 510006, China*

²*School of Computer Science and Engineering, Nanyang Technological University, Singapore 639798, Singapore*

³*Department of Electrical and Computer Engineering, University of Manitoba, Winnipeg, MB R3T 2N2, Canada*

⁴*Department of Electrical and Computer Engineering, Sungkyunkwan University, Suwon 16419, South Korea*

Abstract The emergence of 6G-enabled vehicular metaverses enables Autonomous Vehicles (AVs) to operate across physical and virtual spaces through space-air-ground-sea integrated networks. The AVs can deploy Artificial Intelligence (AI) agents powered by large AI models as personalized assistants, on edge servers to support intelligent driving decision making and enhanced on-board experiences. However, such cross-reality interactions may cause serious location privacy risks, as adversaries can infer AV trajectories by correlating the location reported when AVs request Location-Based Services (LBS) in reality with the location of the edge servers on which their corresponding AI agents are deployed in virtuality. To address this challenge, we design a cross-reality location privacy protection framework based on hybrid actions, including continuous location perturbation in reality and discrete privacy-aware AI agent migration in virtuality. In this framework, a new privacy metric, termed cross-reality location entropy, is proposed to effectively quantify the privacy levels of AVs. Based on this metric, we formulate an optimization problem to optimize the hybrid action, focusing on achieving a balance between location protection, service latency reduction, and quality of service maintenance. To solve the complex mixed-integer problem, we develop a novel LLM-enhanced Hybrid Diffusion Proximal Policy Optimization (LHDPPPO) algorithm, which integrates Large Language Model (LLM)-driven informative reward design to enhance environment understanding with double Generative Diffusion Models (GDMs)-based policy exploration to handle high-dimensional action spaces, thereby enabling reliable determination of optimal hybrid actions. Extensive experiments on real-world datasets demonstrate that the proposed framework effectively mitigates cross-reality location privacy leakage for AVs while maintaining strong user immersion within 6G-enabled vehicular metaverse scenarios.

Keywords Location privacy, vehicular metaverse, large AI model, generative diffusion model, 6G networks, agentic AI

Citation Luo X F, He J Y, Kang J W, et al. Cross-reality Location Privacy Protection in 6G-enabled Vehicular Metaverses: An LLM-enhanced Hybrid Generative Diffusion Model-based Approach. *Sci China Inf Sci*, for review

1 Introduction

The vehicular metaverse is a mobility metaverse paradigm blending of reality and virtuality, which is tailored to enhance intelligence and interactivity in vehicular networks [1, 2]. With the advancement of sixth-generation (6G) cellular technology, 6G-enabled vehicular metaverses have emerged to provide ultra-reliable and low-latency connectivity across space-air-ground-sea integrated networks, enabling uninterrupted and high-quality services for on-board users [3]. In this paradigm, due to the limited computing and storage resources of Autonomous Vehicles (AVs), AVs typically deploy Artificial Intelligence (AI) agents powered by large AI models as their personalized assistants on edge servers, where these edge servers can be terrestrial Roadside Units (RSUs) or Low-Earth Orbit (LEO) satellite nodes [4, 5]. By hosting AI agents and executing computation-intensive tasks, these edge servers enable resource-constrained AVs to access large AI model-based services, thereby enhancing driving safety and on-board immersive experience. In this way, AVs exhibit agentic AI characteristics by leveraging perception, reasoning, execution, and continuous learning capabilities to interact with physical and virtual spaces in an iterative and context-aware manner [6].

Although the 6G-enabled vehicular metaverse empowered by agentic AI enables immersive services and intelligent decision making across physical and virtual spaces, privacy risks become more prominent in such tightly coupled cross-reality systems than traditional vehicular networks [7, 8]. Specifically, the immersion of on-board users within

* Corresponding author (email: kavinkang@gdut.edu.cn)

the vehicular metaverse is highly correlated to two key factors, i.e., reported location precision and service response latency [9]. On the one hand, agentic AI-driven AVs in the physical space often request Location-Based Services (LBS) frequently, such as Augmented Reality (AR) navigation and AR interactive games, where higher reported location precision ensures better Quality of Service (QoS) but also incurs a higher risk of location privacy leakage [10]. On the other hand, due to the continuous mobility of AVs, their corresponding AI agents in the virtual space are frequently migrated among edge servers in alignment with physical vehicle movements to maintain physical–virtual synchronization and low-latency service provisioning, which further amplifies privacy risks [2, 11]. Consequently, collusive adversaries can exploit their prior knowledge of AV routine mobility patterns, such as regular commuting routes, to launch inference attacks that jointly reconstruct vehicle trajectories and AI agent migration patterns, thereby accurately tracking target AVs [12]. This cross-reality linkage attack is more severe and harder to mitigate than traditional single-domain privacy attacks, posing substantial threats to the location privacy of on-board users.

Existing research on cross-reality location privacy preservation in vehicular metaverses has primarily focused on anonymity-based schemes [5, 9], which aim to obscure the linkage between vehicle identities and locations. However, these approaches often suffer from significant performance degradation in low-traffic environments and fail to meet the stringent privacy requirements of AVs [13]. These limitations highlight the need for a general solution capable of protecting cross-reality location privacy in 6G-enabled vehicular metaverses. Moreover, most existing location privacy metrics consider only a single dimension, typically confined to the physical space, and therefore cannot accurately capture privacy leakage risks arising from cross-reality interactions. Consequently, a more comprehensive metric is required to effectively evaluate location privacy under cross-reality inference attacks. Furthermore, strengthening privacy protection at a large scale inevitably increases service response latency and degrades QoS, thereby significantly diminishing user immersion in metaverse environments. As a result, achieving an effective balance among cross-reality location privacy protection, latency reduction, and QoS maintenance remains a challenging and open research problem.

To address the above challenges, this paper proposes a user-centric cross-reality location privacy protection framework based on hybrid action decisions, including the continuous location perturbation in reality and discrete privacy-aware AI agent migration in virtuality. The main contributions of this paper are summarized as follows.

- We present a cross-reality location privacy protection **framework** for 6G-enabled vehicular metaverses to mitigate privacy leakage risk caused by spatiotemporal correlations between physical and virtual spaces. The framework integrates a hybrid action **mechanism** that combines continuous location perturbation in reality with discrete privacy-aware AI agent migration in virtuality to preserve the location privacy of agentic AI-driven AVs.
- In the proposed framework, a new privacy **metric** named cross-reality location entropy is designed to quantify the real-time location privacy levels of AVs under cross-reality inference attacks. The metric is derived from a multi-condition Bayesian posterior distribution and captures the uncertainty of actual vehicle locations introduced by hybrid action strategies. Based on this metric, a mixed-integer optimization problem that jointly considers cross-reality location privacy, service response latency, and QoS loss to optimize hybrid action mechanisms is formulated.
- To solve the formulated complex problem in vehicular metaverse environments, we propose a novel **LLM-enhanced Hybrid Diffusion Proximal Policy Optimization (LHDPO) algorithm**, which incorporates Large Language Model (LLM)-driven informative reward design for enhanced environment understanding and Generative Diffusion Model (GDM)-based policy exploration for improved learning performance in high-dimensional action spaces.
- Extensive experiments using real-world taxi mobility and base station datasets demonstrate that the proposed framework achieves superior performance in terms of cross-reality location privacy preservation, immersive services response latency reduction, and QoS maintenance when compared with existing baseline schemes.

2 Related Work

2.1 Location Privacy Protection in Cross-reality Systems

Location privacy protection has become an active research topic in cross-reality systems, where existing solutions are generally classified into encryption-based, anonymization-based, and obfuscation-based schemes [14]. For encryption-based approaches, Liu et al. [15] proposed BlockSC, a blockchain-empowered spatial crowdsourcing framework that preserves location privacy in metaverses through spatial data encryption. Although effective in securing sensitive information, the heavy computational overhead of cryptographic operations limits its suitability for real-time services in 6G-enabled vehicular metaverses. Anonymization-based schemes aim to weaken the association between users and their trajectories by concealing real identities. For instance, Luo et al. [12] developed a dual

pseudonym change scheme to achieve identity anonymization in vehicular metaverses, but its effectiveness degrades in sparse traffic areas, and it cannot fully realize location concealment. Obfuscation-based schemes protect privacy by perturbing reported positions to reduce adversarial inference accuracy. For instance, Wang et al. [16] proposed a perturbed sliding task queue algorithm based on differential privacy to protect sensitive user location information prior to task offloading in a digital twin architecture, yet it considers only physical space location perturbation and neglects interactions in the virtual space. Therefore, there is still a lack of practical solutions that are capable of preserving cross-reality location privacy in 6G-enabled vehicular metaverses.

2.2 Location Privacy Metrics

Location privacy metrics provide quantitative tools for evaluating protection schemes in mobile networks. Emara et al. [17] showed that widely used metrics in VANETs, such as anonymity set size, entropy, and adversary success rate, each capture only a partial aspect of privacy and may yield inconsistent evaluations across scenarios. Li et al. [18] proposed distance and visibility-based metrics for navigation services, but the metrics remain confined to physical trajectories and ignore virtual space privacy leakage. To model inference from service migration, an entropy-based metric proposed in [11] quantifies location uncertainty under MEC service placement, although it considers only location exposure during service migration and neglects sensitive broadcast information in the physical space. More recently, Kang et al. [5] introduced the Degree of Privacy Entropy (DoPE) to assess pseudonym changes in vehicular edge metaverses, yet DoPE targets identity anonymity within pseudonym-based schemes and does not apply to perturbation-based mechanisms. Overall, existing metrics evaluate privacy within a single domain or narrow application scope and cannot capture cross-reality linkability between broadcast messages and metaverse activities, revealing the need for location privacy metrics tailored to 6G-enabled vehicular metaverses.

2.3 Diffusion Model-based Reinforcement Learning for Decision Optimization

Recent progress in GDMs has demonstrated strong potential in solving complex optimization problems. Du et al. [19] surveyed GDM-based Deep Reinforcement Learning (DRL) and presented a power allocation example that GDMs can capture high-dimensional structures and generate high-quality decisions. Building on this insight, Ning et al. [20] proposed a two-level GDM-based soft actor critic framework for effective resource management, but their method supports only a single action type and has limited applicability. Hence, Kang et al. [21] introduced a hybrid GDM-based DRL algorithm for digital twin migration in vehicular metaverses, jointly generating migration and offloading actions. However, their method relies on traditional RL relaxation techniques to handle hybrid actions, which may destabilize learning and cause suboptimal convergence during training. To further improve hybrid action modeling, Wang et al. [22] embedded GDMs into a hybrid proximal policy optimization algorithm through a parameterized action formulation to optimize spectral efficiency in LEO Satellite networks. Although effective for parameterized decision tasks, this structure imposes mutual exclusivity among actions and limits exploration of new hybrid action pairs. Moreover, existing GDM-based DRL algorithms for optimization still depend entirely on manually crafted reward functions, which may neglect the potentially important components in intricate cross-reality environments. These limitations highlight the need for a new GDM-based DRL algorithm that decouples hybrid actions and leverages large AI models to design informative reward functions.

3 Cross-reality Location Privacy Protection Framework in 6G-enabled Vehicular Metaverses

In this section, we propose a cross-reality location privacy framework based on hybrid action mechanisms in 6G-enabled vehicular metaverses. As illustrated in Fig. 1, each AV in reality is associated with an AI agent in virtuality, which is hosted on one of the edge servers. Firstly, the key components of the 6G-enabled vehicular metaverse are described in the network model. Subsequently, the core hybrid action mechanism is presented, focusing on safeguarding location privacy across both physical and virtual spaces.

3.1 Network Model

- **Agentic AI-driven AVs:** Agentic AI-driven AVs operating in the physical space act as primary participants in 6G-enabled vehicular metaverses. Each AV can request customized LBS, such as AR navigation, to enhance the on-board experience throughout the journey. Although these services are essential for user immersion, the associated service requests inevitably disclose sensitive location information, which can be exploited by adversaries to track AV movements [10].

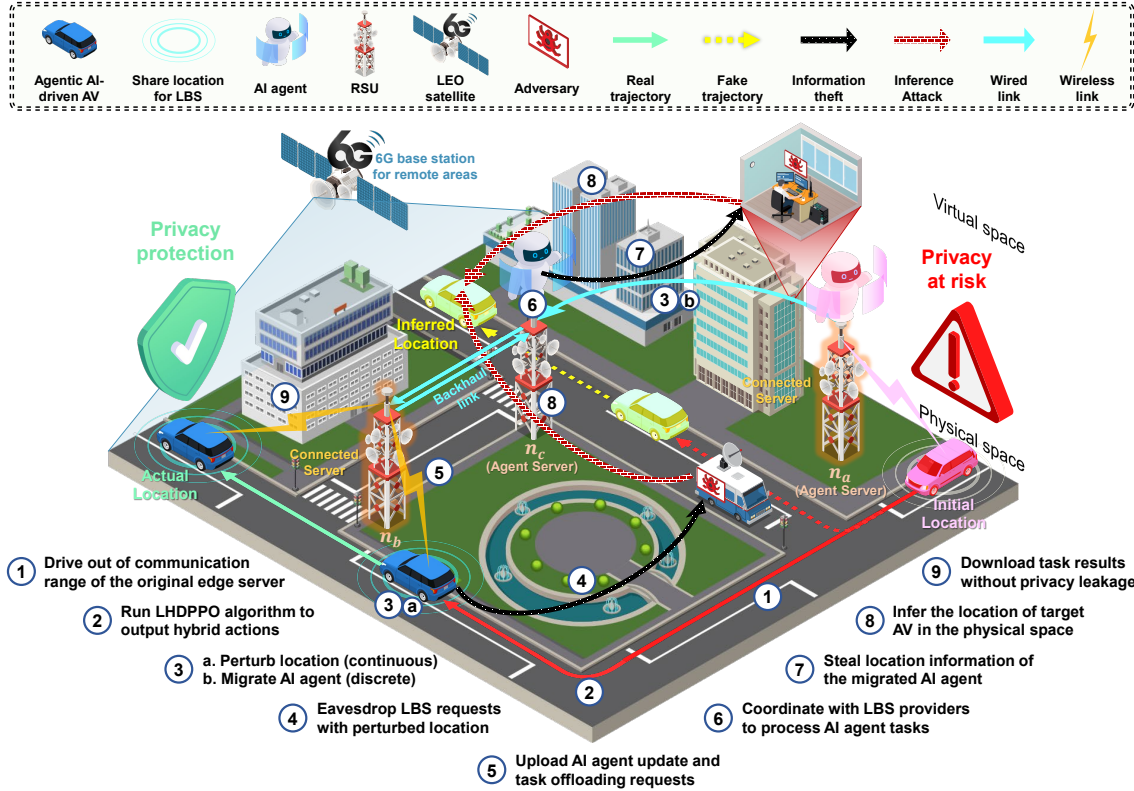


Figure 1 Workflow of the proposed cross-reality location privacy protection framework based on hybrid actions in 6G-enabled vehicular metaverses. The sequentially numbered arrows depict the main processes: (a) The target AV at privacy risks moves and executes hybrid actions, i.e., the continuous location perturbation and discrete privacy-aware AI agent migration (Steps ① to ③). (b) The AV requests LBS and offloads AI agent tasks to edge servers, while malicious adversaries exploit the illegally obtained information of the target AV to launch inference attacks (Steps ④ to ⑧). (c) The on-board user obtains immersive metaverse applications without compromising location privacy (Step ⑨).

- **AI agents:** AI agents residing in the virtual space act as intelligent assistants for their corresponding AVs. By directly interacting with other AI agents and LBS providers, AI agents empowered by large AI models can assist AVs in processing computation-intensive tasks and providing decision-support functionalities. However, frequent interactions and continuous migrations of AI agents may inadvertently leak location-related information [12]. To tackle the privacy threats, the large AI model-based AI agents can support AVs with agentic AI capacities to determine hybrid actions for cross-reality location privacy protection.

- **Edge Servers:** Edge servers function as the bridge between the physical and virtual spaces in 6G-enabled vehicular metaverses. Equipped with larger computing and storage resources than AVs, they manage the full lifecycle of AI agents, including creation, synchronization, execution, and migration. In the 6G-enabled vehicular metaverse, edge servers can be terrestrial RSUs or LEO satellites, where satellite nodes act as 6G base stations to compensate for poor terrestrial connectivity in remote areas [23].

- **Adversaries:** Adversaries may exist in both physical and virtual spaces and are considered to possess prior knowledge about target AVs. This consideration is reasonable, as the driving route and social interaction pattern of an AV often exhibit temporal regularity [11]. In the physical space, adversaries can eavesdrop on broadcast sensitive information of AVs when they request LBS. In the virtual space, adversaries may be malicious AI agents or metaverse service providers aiming to infer user locations, particularly during AI agent migrations. Furthermore, adversaries across physical and virtual spaces may share information to launch collusive inference attacks to associate an AV with its AI agent, posing a significant threat to the location privacy of on-board users [12].

3.2 Hybrid Action-based Cross-reality Privacy Protection Mechanism

To conceal user location in 6G-enabled vehicular metaverses, the proposed cross-reality location privacy protection framework adopts a hybrid action mechanism consisting of a continuous action for location perturbation in the physical space and a discrete action for privacy-aware AI agent migration in virtual spaces. See the details below.

3.2.1 Continuous action—location perturbation in reality

We consider there are multiple agentic AI-driven AVs, multiple RSUs, and an LEO satellite in an observation area. Specifically, we denote an AV set $\mathbb{M} = \{1, \dots, m, \dots, M\}$ with a total of M AVs and an RSU set $\mathbb{N} = \{1, \dots, n, \dots, N\}$ with a total of N RSUs, while the index of the LEO satellite is denoted as S . In the physical space, location perturbation (also called location obfuscation) can be applied to AV trajectories to reduce the risk of direct location exposure [13]. Each AV introduces controlled perturbations to its reported coordinates when requesting LBS. Notably, larger perturbations increase privacy by enlarging the uncertainty of an adversary's inference but also weaken QoS [10]. Hence, the perturbation intensity can be modeled as a continuous action variable that is adjusted based on the privacy and QoS requirements of AVs.

The planar Laplacian perturbation mechanism proposed in [24] provides a principled approach to achieving geo-indistinguishability based on differential privacy. This method samples random noise from a two-dimensional Laplace distribution and perturbs the original location to satisfy ϵ -geo-indistinguishability, where ϵ denotes the privacy budget. Inspired by this approach, the proposed framework adopts a similar mechanism to implement continuous location perturbation in the physical space.

Let $l_m^t = (x_m^t, y_m^t)$ denote the true location of AV m at time slot t , where x_m^t and y_m^t represent the longitude and latitude, respectively. In a polar coordinate system centered at l_m^t , any relative location l_x can be represented as (r_m^t, θ_m^t) , where r_m^t denotes the perturbation radius and θ_m^t denotes the perturbation angle with respect to the horizontal axis. According to [24], the Probability Density Function (PDF) of the polar Laplacian distribution is

$$D_\epsilon(r_m^t, \theta_m^t) = \frac{\theta_m^t}{2\pi} r_m^t e^{-\epsilon r_m^t}. \quad (1)$$

Eq. (1) reflects that perturbation is jointly determined by the continuous random variables r_m^t and θ_m^t . Hence, to perform location perturbation at time slot t , AV m only needs to select a continuous action policy $\mathbf{c}_m^t = \{r_m^t, \theta_m^t\}$. Given the selected r_m^t and $\theta_m^t \in [0, 2\pi)$, the perturbed location \tilde{l}_m^t is computed as

$$\tilde{l}_m^t = (\tilde{x}_m^t, \tilde{y}_m^t) = (x_m^t + r_m^t \cos \theta_m^t, y_m^t + r_m^t \sin \theta_m^t). \quad (2)$$

The detailed procedure for determining \mathbf{c}_m^t with the LLM-enhanced learning approach is presented in Section 5.

3.2.2 Discrete action—privacy-aware AI agent migration in virtuality

In the virtual domain, AI agent migration serves not only to sustain continuous service provisioning under the mobility of AVs, but also as an effective mechanism for enhancing location privacy [11]. By dynamically changing the hosting edge server of an AI agent, the one-to-one correspondence between an AV and a specific server can be disrupted, thereby introducing uncertainty into the inferred locations of AVs and reducing privacy risks. However, if an AV always migrates its AI agent to the server offering the strongest signal strength, an adversary continuously monitoring the target AI agent can still reconstruct the real trajectory of the target AV. Conversely, migrating the AI agent to a distant edge server may increase service response latency and degrade user immersion in 6G-enabled vehicular metaverses. To address this tradeoff, privacy-aware AI agent migration is modeled as a discrete action, where an AV optimally selects whether and where to migrate its agent among edge server candidates, achieving a dynamic balance between location privacy protection and service latency reduction.

Let c_m^t denote the index of the edge server connected to AV m at time slot t . In a 6G-enabled vehicular metaverse, each AV is connected to exactly one edge server in each time slot, which is expressed as $\mathbb{1}(c_m^t \in \mathbb{N}) + \mathbb{1}(c_m^t = S) = 1$, where $\mathbb{1}(\cdot)$ is the indicator function. Meanwhile, let e_m^t denote the index of the edge server that hosts the AI agent of AV m , referred to as the agent server. As illustrated in Fig. 1, the glowing RSU $n_a \in \mathbb{N}$ represents the edge server providing the strongest signal to AV m at its initial position, serving both as the connected edge server and the initial agent server. When AV m moves out of the coverage range of RSU n_a , it connects to another RSU $n_b \in \mathbb{N}$ that offers the strongest signal at the new position. However, the connected server n_b is not necessarily selected as the agent server. After evaluating the current location privacy level, AV m may instead choose an alternative RSU n_c ($n_c \in \mathbb{N}$) to balance privacy protection and service latency based on its discrete action decision policy $\mathbf{d}_m^t = n_c$.

Therefore, to protect location privacy in the virtual space, the agentic AI-driven AV m can determine its discrete action policy $\mathbf{d}_m^t = \{e_m^t \mid \mathbb{1}(e_m^t \in \mathbb{N}) + \mathbb{1}(e_m^t = S) = 1\}$ for privacy-aware AI agent migration in time slot t . The detailed procedure for determining \mathbf{d}_m^t with the LLM-enhanced learning approach is presented in Section 5.

4 System Model

Based on the above analysis, the core of the proposed framework for achieving cross-reality location privacy protection is to determine the optimal hybrid action, striking a balance between location privacy protection and user immersion. To achieve this, we design a new privacy metric named cross-reality location entropy to evaluate privacy levels under the hybrid action mechanisms. Meanwhile, the service response latency and QoS loss are explicitly modeled. By integrating these components, the overall optimization problem is formulated in Section 4.4.

4.1 New Privacy Metric: Cross-reality Location Entropy

Before determining the hybrid action for cross-reality location privacy protection, it is essential for AV m to evaluate its current privacy level. When the assessed privacy level is high, AV m can prioritize its immersive experience within the metaverse, meaning that it can request LBS with accurate locations and deploy its AI agent on a nearby edge server. In contrast, AV m can adopt a more aggressive protection strategy, requesting LBS with largely perturbed positions and migrating its AI agent to a more distant edge server.

As discussed in Section 3.1, adversaries can obtain partial historical movement trajectories of target AVs. With this side information, an adversary can analyze the migration pattern of the target AV and conduct a Bayesian location inference attack, which is a type of knowledge-based attack [11]. Combining past movement traces and migration patterns, adversaries can build a mapping relationship between AV location in reality and AI agent location in virtuality, learning the probability distribution of the AV's real-time actual position. Specifically, let $\Pr(\check{l}_m^t = p_a)$, $\Pr(\check{l}_m^t = p_b)$, and $\Pr(\hat{l}_m^t = p_c)$ represent the probability of the inferred AV location, perturbed AV location, and corresponding AI agent location of AV m is located at the position p_a , p_b , and p_c , respectively. Then, the posterior distribution of AV m 's location is obtained by observing the perturbed AV location in reality and the AI agent location in virtuality based on the multi-condition Bayes' theorem, given by

$$\Pr(\check{l}_m^t = p_a | \check{l}_m^t = p_b, \hat{l}_m^t = p_c) = \frac{\Pr(\check{l}_m^t = p_a, \check{l}_m^t = p_b, \hat{l}_m^t = p_c)}{\Pr(\check{l}_m^t = p_b, \hat{l}_m^t = p_c)} = \frac{\Pr(\check{l}_m^t = p_b, \hat{l}_m^t = p_c | \check{l}_m^t = p_a) \Pr(\check{l}_m^t = p_a)}{\sum_{p_x \in \mathcal{P}_m^t} \Pr(\check{l}_m^t = p_b, \hat{l}_m^t = p_c | l_m^t = p_x) \Pr(l_m^t = p_x)}, \quad (3)$$

where \mathcal{P}_m^t is the set of potential physical locations of AV m in time slot t . Since the perturbed location and AI agent location are each determined solely based on the hybrid action strategy of AV m , the two conditional probabilities can be treated as mutually independent when the physical AV location is given. In this case, the posterior distribution in Eq. (3) is transformed into

$$\Pr(\check{l}_m^t = p_a | \check{l}_m^t = p_b, \hat{l}_m^t = p_c) = \frac{\Pr(\check{l}_m^t = p_b | \check{l}_m^t = p_a) \Pr(\hat{l}_m^t = p_c | \check{l}_m^t = p_a) \Pr(\check{l}_m^t = p_a)}{\sum_{p_x \in \mathcal{P}_m^t} \Pr(\check{l}_m^t = p_b | l_m^t = p_x) \Pr(\hat{l}_m^t = p_c | l_m^t = p_x) \Pr(l_m^t = p_x)}. \quad (4)$$

To assess the privacy levels of AVs in 6G-enabled vehicular metaverses, we design a new physical-virtual location privacy metric based on information entropy, referred to as cross-reality location entropy.

Definition 1. (Cross-reality Location Entropy) *In the 6G-enabled vehicular metaverse, the cross-reality location entropy of an AV m at time slot t is defined as*

$$E_m^t = - \sum_{p_a \in \mathcal{P}_m^t} \Pr(\check{l}_m^t = p_a | \check{l}_m^t = p_b, \hat{l}_m^t = p_c) \log_2 \left(\Pr(\check{l}_m^t = p_a | \check{l}_m^t = p_b, \hat{l}_m^t = p_c) \right). \quad (5)$$

Notably, the cross-reality location entropy in Eq. (5) is established based on the concept of entropy in information theory [25]. A larger entropy value implies a lower accuracy of the adversary's inference regarding the actual location of the target AV, indicating a lower risk of location privacy leakage. With this metric, AVs can evaluate their location privacy levels across physical and virtual spaces, thereby guiding hybrid action mechanisms to maintain an appropriate balance between location privacy and user immersion in 6G-enabled vehicular metaverses.

4.2 Service Response Latency Model

4.2.1 Communication model

The communication model describes the wireless transmission processes between AVs and edge servers. To maintain accurate physical-virtual synchronization and receive high-quality metaverse services, AVs should upload real-time sensing data to edge servers for updating their Large AI model-empowered AI agents and offloading computation

tasks through uplink channels [9]. Consider the case where the AI agent of AV m is deployed on RSU n in the virtual space during time slot t , i.e., $e_m^t = n$. Let $\hat{l}_m^t = l_n = \{x_n, y_n\}$ denote the position of agent server e_m^t , which corresponds to the fixed geographical coordinates of RSU n , with x_n and y_n representing its longitude and latitude, respectively. The longitudinal difference between AV m and RSU n is thus given by $\Delta x_{m,n}^t = \frac{\pi}{180} (x_m^t - x_n)$, while the latitudinal difference is $\Delta y_{m,n}^t = \frac{\pi}{180} (y_m^t - y_n)$. Therefore, the haversine of the central angle $\theta_{m,n}^t$ (in radians) is

$$\text{hav}(\theta_{m,n}^t) = \sin^2\left(\frac{\theta_{m,n}^t}{2}\right) = \sin^2(\Delta x_{m,n}^t) + \cos(\frac{\pi}{180} y_m^t) \cos(\frac{\pi}{180} y_n) \sin^2(\Delta y_{m,n}^t). \quad (6)$$

From Eq. (6), we know that $\theta_{m,n}^t = 2 \arcsin \sqrt{\text{hav}(\theta_{m,n}^t)}$. Then, the actual distance between AV m and RSU n is

$$d_{m,n}^t = R\theta_{m,n}^t = 2R \arcsin \sqrt{\text{hav}(\theta_{m,n}^t)}, \quad (7)$$

where $R = 6371$ km denotes the radius of the Earth.

For vehicular systems, the Rayleigh fading model is commonly used to characterize the wireless channel between RSUs and AVs [2]. The channel gain is defined as $h_{m,n}^t = A \left[\frac{c}{4\pi f_c d_{m,n}^t} \right]^\xi$, where $c = 3 \times 10^8$ m/s is the speed of light, A is the antenna gain, f_c is the carrier frequency, and ξ is the path loss factor [2]. Therefore, the achievable uplink data rate from AV m to the server c_m^t is

$$R_{m,n}^{\text{up}}(t) = B_{m,n}^{\text{up}} \log_2 \left(1 + \frac{p_m h_{m,n}^t}{N_0} \right), \quad (8)$$

where $B_{m,n}^{\text{up}}$ is the uplink bandwidth allocated to AV m when connected to RSU n , p_m is the transmit power of AV m , and N_0 is the average noise power. Considering two types of edge servers, the uplink communication latency is

$$L_m^{\text{up}}(t) = \mathbb{1}(c_m^t \in \mathbb{N}) \frac{D_m^{\text{up}}(t)}{R_{m,n}^{\text{up}}(t)} + \mathbb{1}(c_m^t = S) \frac{D_m^{\text{up}}(t)}{R_{\text{sat}}^{\text{up}}}, \quad (9)$$

where $D_m^{\text{up}}(t)$ is the amount of data uploaded by AV m for AI agent updates and task offloading, and $R_{\text{sat}}^{\text{up}}$ denotes the average ground-to-satellite upload speed in Starlink¹⁾.

In addition to uplink transmission, AVs also receive customized AI agent task results from the RSU via the downlink channel to obtain personalized metaverse services (e.g., AR navigation to a preferred destination). Considering channel reciprocity, the uplink and downlink share identical path-loss characteristics [21]. Accordingly, the downlink data rate is $R_{m,n}^{\text{down}}(t) = B_{m,n}^{\text{down}} \log_2 \left(1 + \frac{p_n h_{m,n}(t)}{N_0} \right)$, where $B_{m,n}^{\text{down}}$ denotes the downlink bandwidth allocated to AV m when connected to edge server c_m^t , and p_n is transmit power of RSU n . To receive AI agent task results of size $D_m^{\text{down}}(t)$, the downlink communication latency in time slot t is given by

$$L_m^{\text{down}}(t) = \mathbb{1}(c_m^t \in \mathbb{N}) \frac{D_m^{\text{down}}(t)}{R_{m,n}^{\text{down}}(t)} + \mathbb{1}(c_m^t = S) \frac{D_m^{\text{down}}(t)}{R_{\text{sat}}^{\text{down}}}, \quad (10)$$

where $R_{\text{sat}}^{\text{down}}$ denotes the average ground-to-satellite download speed in Starlink¹⁾.

Since the connected edge server may differ from the agent server, the communication model also accounts for the backhaul latency incurred during data transmission between them. This latency only arises in ground-to-ground RSU links, as satellite nodes typically possess sufficient onboard computing resources, eliminating the need for AVs connected to satellites to offload AI agent tasks to terrestrial RSUs. The backhaul latency consists of two components: the wired transmission latency and the relay latency, where the latter is influenced by processing, forwarding, and queuing delays along the relay path. Therefore, the backhaul latency is expressed as

$$L_m^{\text{back}}(t) = \mathbb{1}(e_m^t = n) \left(\mathbb{1}(c_m^t \neq e_m^t) \frac{D_m^{\text{up}}(t) + D_m^{\text{down}}(t)}{R_N} + 2\varphi_t^{\text{back}} d_{c_m^t \rightarrow e_m^t} \right). \quad (11)$$

Here, R_N is the wired transmission rate between RSUs for AI agent migrations, φ_t^{back} is a positive coefficient of the backhaul latency, and $d_{c_m^t \rightarrow e_m^t}$ is the hop count between the connected edge server c_m^t and the agent server e_m^t .

Finally, the total communication latency is calculated by

$$L_m^{\text{comm}}(t) = L_m^{\text{up}}(t) + L_m^{\text{back}}(t) + L_m^{\text{down}}(t). \quad (12)$$

1) <https://www.starlink.com/technology>

4.2.2 Migration model

According to Section 3.2.2, a moving AV m executes a discrete action, namely privacy-aware AI agent migration, to balance location privacy and service latency, which introduces migration latency. Let S_m denote the AI agent model size of AV m . The incurred migration latency of AV m between the previous agent server and the current one is then computed as

$$L_m^{\text{mig}}(t) = \begin{cases} 0, & e_m^t = e_m^{t-1}, \\ \frac{S_m}{R_N} + \varphi^{\text{mig}} d_{e_m^{t-1} \rightarrow e_m^t}, & e_m^t = n, e_m^{t-1} \in (\mathbb{N} \setminus \{n\}), \\ \frac{S_m}{R_{\text{sat}}^{\text{up}}}, & e_m^t = S, e_m^{t-1} \in \mathbb{N}, \\ \frac{S_m}{R_{\text{sat}}^{\text{down}}}, & e_m^t \in \mathbb{N}, e_m^{t-1} = S, \end{cases} \quad (13)$$

where φ^{mig} denotes the RSU-to-RSU AI migration latency coefficient.

4.2.3 Computation model

In addition to wireless communication and migration operations, the process of delivering metaverse services to AVs by AI agents also incurs computation latency at the agent server. Specifically, the agent server e_m^t is responsible for AI agent updates and task processing for the agentic AI-driven AV m , resulting in the computation latency as

$$L_m^{\text{comp}}(t) = \mathbb{1}(e_m^t \in \mathbb{N}) \frac{c_m D_m^{\text{task}}(t)}{f_n} + \mathbb{1}(e_m^t = S) \frac{c_m D_m^{\text{task}}(t)}{f_{\text{sat}}}. \quad (14)$$

Here, c_m is the number of Central Processing Unit (CPU) cycles to process per unit data uploaded from AV m (in CPU Cycles/bit), and $D_m^{\text{task}}(t) = \iota D_m^{\text{up}}(t)$ is the size of the requested AI agent task created based on the upload data with ι denoting the conversion factor. f_n and f_{sat} are the CPU frequency of RSU n and satellite S , respectively.

Finally, by integrating the communication latency, migration latency, and computation latency, the total service response latency experienced by AV m in time slot t is expressed as

$$L_m^t = L_m^{\text{comm}}(t) + L_m^{\text{mig}}(t) + L_m^{\text{comp}}(t). \quad (15)$$

4.3 Penalties for QoS Loss

QoS is another critical requirement in 6G-enabled vehicular metaverses. When agentic AI-driven AVs travel and request splendid LBS, injecting excessive noise into their status messages can decline the QoS, thus leading to poor metaverse experiences, such as offset scenario rendering and improper site recommendation. To prevent such situations, a penalty term for QoS loss regarding the distance between the actual and perturbed locations is introduced to constrain large-scale continuous actions. According to Eq. (2), the perturbed location of AV m after applying the continuous action is $\tilde{l}_m^t = (\tilde{x}_m^t, \tilde{y}_m^t)$. Referring to the distance calculation formula in Eq. (7), we define the penalty for QoS loss as

$$Q_m^t = \ln \left(1 + 2R \arcsin \sqrt{\sin^2 \left(\frac{\pi}{180} (x_m^t - \tilde{x}_m^t) \right) + \cos \left(\frac{\pi}{180} y_m^t \right) \cos \left(\frac{\pi}{180} \tilde{y}_m^t \right) \sin^2 \left(\left(\frac{\pi}{180} (y_m^t - \tilde{y}_m^t) \right) \right)} \right). \quad (16)$$

4.4 Problem Formulation

Generally, the proposed framework requires each agentic AI-driven AV to determine how to perturb its physical location and migrate its AI agent to protect cross-reality location privacy and ensure user immersion by maintaining service response latency and QoS. Consequently, the utility function of AV m is defined as

$$u_m^t = \omega_E E_m^t - \omega_L L_m^t - \omega_Q Q_m^t, \quad (17)$$

where ω_E , ω_L , and ω_Q represent the weighting factors for the cross-reality location entropy, service response latency, and QoS loss, respectively. Finally, the overall optimization problem of the proposed hybrid action mechanisms in the 6G-enabled vehicular metaverse is formulated as

$$\mathbf{P1} : \max_{r_m^t, \theta_m^t, e_m^t} \frac{1}{T} \frac{1}{M} \sum_{t=1}^T \sum_{m=1}^M u_m^t, \quad (18a)$$

$$\text{s.t. } r_m^t \in [0, r_{\max}], \quad (18b)$$

$$\theta_m^t \in [0, 2\pi], \quad (18c)$$

$$\mathbb{1}(e_m^t \in \mathbb{N}) + \mathbb{1}(e_m^t = S) = 1. \quad (18d)$$

Here, r_{\max} is the maximum perturbation radius of AVs. Constraints (18b), (18c) and (18d) limit the value ranges of the optimization variables. It is observed that the formulated problem **P1** is a complex non-convex mixed-integer programming problem. Since cross-reality location privacy preservation is persistent and varies over time, traditional convex optimization methods that provide only single-round static solutions are often invalid. Moreover, the long-term coupling among consecutive decisions in dynamic vehicular metaverse scenarios makes learning-based methods more suitable than conventional optimization for achieving sustained privacy and immersion performance.

5 LLM-enhanced Hybrid GDM-based Reinforcement Learning Solution

Although it is difficult to solve the optimization problem directly, the problem **P1** exhibits a memoryless sequential decision-making structure that satisfies the Markov property. Based on this observation, we model the hybrid action decision process as a Markov Decision Process (MDP) [11]. Moreover, large AI models exhibit a strong ability to understand contextual information in highly dynamic systems, among which LLMs are particularly effective at reasoning over abstract objectives and discovering latent performance indicators. Motivated by recent advances in LLM-enhanced reinforcement learning [26], we propose an LLM-enhanced Hybrid Diffusion-based Proximal Policy Optimization (LHDPO) algorithm to solve the complex optimization problem **P1**.

5.1 Markov Decision Process Modeling

5.1.1 Environment state

Let \check{l}_m^t denote the position of the connected server c_m^t . Thus, the state space of AV m in the current time slot $t \in \{1, 2, \dots, T\}$ is defined as a union of the real-time vehicle location l_m^t , the location of the connected edge server \check{l}_m^t , and the location of the edge server hosting the AI agent in the previous slot \hat{l}_m^{t-1} , which is represented by

$$s_m^t \triangleq \{l_m^t, \dot{\theta}_m^t, \check{l}_m^t, \hat{l}_m^{t-1}\}. \quad (19)$$

Therefore, the state space in the MDP is the aggregation of the states of all AVs, denoted as $\mathbf{s}^t = \{s_m^t\}_{m=1}^M$.

5.1.2 Action space

At each time slot t , each agentic AI-driven AV autonomously determines a hybrid action, consisting of a set of continuous action \mathbf{a}_m^t including the perturbation radius r_m^t and perturbation angle θ_m^t in reality, and a discrete action \mathbf{d}_m^t , i.e., the AI agent migration decision e_m^t in virtuality. Therefore, the action of AV m is denoted as $\mathbf{a}_m^t \triangleq \{c_m^t, \mathbf{d}_m^t\} = \{r_m^t, \theta_m^t, e_m^t\}$. Consequently, the action space in the MDP is defined as $\mathbf{a}^t = \{\mathbf{c}^t, \mathbf{d}^t\} = \{\mathbf{a}_m^t\}_{m=1}^M$.

5.1.3 Reward function

The reward function characterizes the immediate feedback received by AVs after executing the hybrid action \mathbf{a}^t under the environment state \mathbf{s}^t , which plays a vital role in guiding policy updates in MDP. A well-designed reward function should accurately reflect the system objective and provide informative gradients to facilitate stable and reliable policy updates. Intuitively, assigning the reward to be directly equal to the utility of AVs encourages the policy network to generate hybrid actions that jointly enhance location privacy, latency, and QoS performance. Following this principle, the reward function is designed as

$$\mathcal{R}_{\text{man}}(\mathbf{s}^t, \mathbf{a}^t) = \frac{1}{M} \sum_{m=1}^M u_m^t. \quad (20)$$

However, such manually crafted rewards are often limited to predefined objective terms and penalty components, and may fail to capture implicit interactions among location privacy, service response latency, and QoS in the complex cross-reality vehicular metaverse scenario, potentially leading to suboptimal convergence.

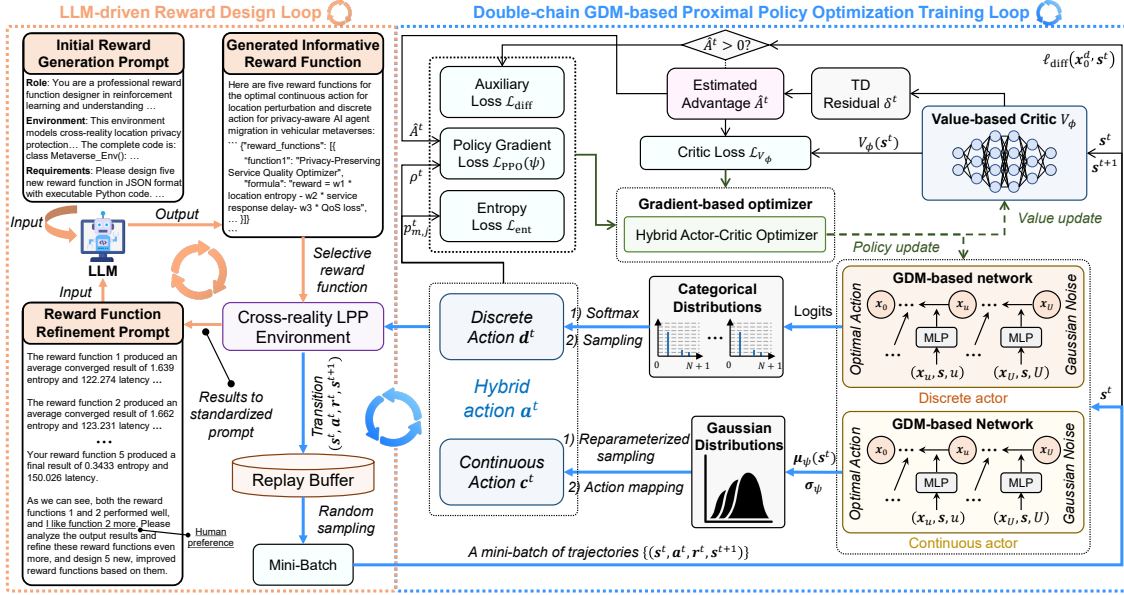


Figure 2 Architecture of the proposed LHDPPPO algorithm for the cross-reality Location Privacy Protection (LPP) environment.

5.2 LHDPPPO Algorithm Details

5.2.1 LLM-driven reward function design loop

Instead of relying solely on manual formulations that may neglect the important environmental components, the proposed LHDPPPO algorithm employs an LLM as an autonomous reward designer to generate more informative reward functions. This design philosophy is consistent with the role of agentic AI, where the LLM is integrated into the reinforcement learning loop to enhance policy learning through adaptive reward shaping.

As illustrated in Fig. 2, the LLM-driven reward design follows an iterative loop consisting of three main stages.

Stage 1: Initial reward generation: The LLM is first prompted with three categories of inputs to produce a set of candidate reward functions. These inputs include

- Role assignment: The prompt instructs the LLM to act as an experienced and professional reward designer with expertise in wireless communications, security and privacy, and deep reinforcement learning.
- Environment description: The prompt provides a detailed description of the 6G-enabled vehicular metaverse scenario together with the complete environment code, including the MDP formulation and parameter configuration.
- Output specification: The prompt requires the LLM to generate reward functions in a structured JSON format, accompanied by executable Python code that can be directly integrated into the simulation environment.

Stage 2: Selective reward evaluation: Based on the generated candidate reward functions, domain experts selectively retain those that are suitable for training and discard unreasonable ones, such as functions that assign excessive weight to a single term. Each retained reward function is then evaluated through interactions with the environment, and key performance indicators such as achieved location entropy and service latency are collected.

Stage 3: Circular reward refinement: The evaluation results from Stage 2 are standardized and fed back to the LLM as refinement prompts. Guided by explicit performance comparisons and optional human preferences, the LLM iteratively updates and improves the reward formulations by emphasizing influential components that are often overlooked in manual designs, such as the coupled effects of privacy, latency, and QoS. This closed reward design loop continues until convergence to a high-performing reward function, as shown on the left of Fig. 2.

After multiple refinement rounds, the LLM outputs the most informative reward function for cross-reality location privacy protection, which is finally adopted by the learning agent:

$$r^t = \mathcal{R}_{\text{LLM}}(s^t, a^t) = \frac{1}{M} \sum_{m=1}^M \left(\omega_1 E_m^t - \omega_2 \ln(1 + L_m^t) - \omega_3 \hat{Q}_m^t - \omega_4 \ln(1 + d_{m, e_m^t}^t) + \omega_5 \alpha_m^t \right). \quad (21)$$

Here, $\hat{Q}_m^t = \frac{Q_m^t}{Q_{\max}}$ is the normalized QoS loss, with Q_{\max} representing the maximum QoS loss under the maximum perturbation radius r_{\max} . $d_{m, e_m^t}^t$ is the distance between the AV m and the selected agent server e_m^t . α_m^t is the included angle between the vehicle-to-server direction and perturbation direction. $\omega_1, \omega_2, \omega_3, \omega_4$, and ω_5 are

the optimized weighting factors obtained through multiple rounds of LLM-guided reward refinement, which yield superior learning performance. Compared with $\mathcal{R}_{\text{man}}(\cdot)$, the LLM-generated reward incorporates latent yet critical indicators and explicitly balances location privacy with user immersion, enabling the proposed LHDPPPO algorithm to better improve policy robustness and convergence performance in 6G-enabled vehicular metaverses.

5.2.2 Double-chain GDM-based PPO training loop

Beyond the LLM-driven reward design, the proposed LHDPPPO algorithm integrates powerful GDMs that can model complex, high-dimensional distributions through multi-step denoising processes, enabling structured action exploration in the highly coupled decision space of 6G-enabled vehicular metaverses. Specifically, LHDPPPO leverages two diffusion policies to handle continuous and discrete actions, respectively, jointly forming the hybrid policy as

$$\pi_{\psi}(\mathbf{a}^t | \mathbf{s}^t) = \pi_{\psi^c}^c(\mathbf{c} | \mathbf{s}^t) \pi_{\psi^d}^d(\mathbf{d} | \mathbf{s}^t), \quad (22)$$

where $\mathbf{c} = \{\epsilon_m, \theta_m\}_{m=1}^M$ denotes the continuous actions for location perturbation and $\mathbf{d} = \{e_m\}_{m=1}^M$ denotes the discrete actions for privacy-aware AI agent migration. The key idea of GDM-based algorithms is to exploit the reverse diffusion process to progressively refine actions from noise into feasible solutions, thereby enabling effective exploration for near-optimal hybrid actions. This generative denoising process is conceptually described as

$$p_{\psi}(\mathbf{x}_{0:U} | \mathbf{s}) = \mathcal{N}(\mathbf{x}_U; \mathbf{0}, \mathbf{I}) \prod_{u=1}^U p_{\psi}(\mathbf{x}_{u-1} | \mathbf{x}_u, \mathbf{s}), \quad (23)$$

where U is the number of denoising steps, \mathbf{I} is the covariance matrix, and \mathbf{x}_0 is the final output of the reverse chain.

The reverse diffusion chain $\{p_{\psi}(\mathbf{x}_{u-1} | \mathbf{x}_u, \mathbf{s})\}_{u=1}^U$ is modeled as a sequence of conditional Gaussian transitions,

$$p_{\psi}(\mathbf{x}_{u-1} | \mathbf{x}_u, \mathbf{s}) = \mathcal{N}(\mathbf{x}_{u-1}; \boldsymbol{\mu}_{\psi}(\mathbf{x}_u, \mathbf{s}, u), \boldsymbol{\Sigma}_{\psi}(\mathbf{x}_u, \mathbf{s}, u)), \quad (24)$$

where the covariance follows a predefined variance schedule $\boldsymbol{\Sigma}_{\psi}(\mathbf{x}_u, \mathbf{s}, u) = \beta_u \mathbf{I}$ and the mean is parameterized via the noise prediction network $\boldsymbol{\epsilon}_{\psi}$ as

$$\boldsymbol{\mu}_{\psi}(\mathbf{x}_u, \mathbf{s}, u) = \frac{1}{\sqrt{\alpha_u}} \left(\mathbf{x}_u - \frac{\beta_u}{\sqrt{1 - \bar{\alpha}_u}} \boldsymbol{\epsilon}_{\psi}(\mathbf{x}_u, \mathbf{s}, u) \right), \quad (25)$$

with $\alpha_u = 1 - \beta_u$ and $\bar{\alpha}_u = \prod_{k=1}^u \alpha_k$.

Accordingly, the hybrid policy $\pi_{\psi}(\mathbf{a}^t | \mathbf{s}^t)$ is realized by executing the reverse diffusion process from $\mathbf{x}_U \sim \mathcal{N}(\mathbf{0}, \mathbf{I})$ to \mathbf{x}_0 , where the final denoised sample \mathbf{x}_0 corresponds to the executed action \mathbf{a}^t . The same reverse diffusion principle is applied to both continuous and discrete components, yielding \mathbf{c} and \mathbf{d} , respectively. Consequently, optimizing the policy π_{ψ} in the high-dimensional vehicular metaverse environment is equivalent to optimizing the denoising networks $\boldsymbol{\epsilon}_{\psi^c}^c$ and $\boldsymbol{\epsilon}_{\psi^d}^d$ that govern the reverse diffusion dynamics of the continuous and discrete action spaces. These denoising networks fully determine the action distribution and finally the behavior of the learning agent.

At time slot t , the hybrid log-probability of the executed action generated by the diffusion policy is computed as

$$\log \pi_{\psi}(\mathbf{a}^t | \mathbf{s}^t) = \log \pi_{\psi^c}^c(\mathbf{c}^t | \mathbf{s}^t) + \log \pi_{\psi^d}^d(\mathbf{d}^t | \mathbf{s}^t). \quad (26)$$

In LHDPPPO, both the continuous and discrete policies are implemented by diffusion-based actors that execute the reverse diffusion chain in a mean-only denoising mode. The stochasticity required for policy optimization is solely introduced by the final distributions, which ensures tractable likelihood evaluation and stable PPO updates.

For the continuous component, the diffusion actor produces a mean $\boldsymbol{\mu}_{\psi^c}(\mathbf{s}^t)$, and the continuous policy is then modeled as a Gaussian distribution, given by

$$\pi_{\psi^c}^c(\mathbf{c}^t | \mathbf{s}^t) = \mathcal{N}(\mathbf{c}^t; \boldsymbol{\mu}_{\psi^c}(\mathbf{s}^t), \text{diag}(\boldsymbol{\sigma}_{\psi^c}^2)), \quad (27)$$

where the log-variance vector $\boldsymbol{\sigma}_{\psi^c}$ is learned jointly with the diffusion model parameters. This construction enables the PPO policy gradient to propagate through the log-probability of the sampled action into the continuous denoising network $\boldsymbol{\epsilon}_{\psi^c}^c$, thereby shaping the reverse diffusion dynamics according to long-term system performance.

For the discrete component, a diffusion-based denoising network generates the categorical logits for each AV, from which the migration action e_m^t is sampled. Then, the corresponding log-probability is computed by

$$\log \pi_{\psi^d}^d(\mathbf{d}^t | \mathbf{s}^t) = \sum_{m=1}^M \log \text{Cat}(e_m^t | \text{logits}_m(\mathbf{s}^t)). \quad (28)$$

The gradients of this log-probability propagate through the diffusion-generated logits and update the discrete denoising network $\epsilon_{\psi^d}^d$, thereby completing the coupling between diffusion modeling and PPO-based policy optimization.

For PPO updates, we denote $\pi_{\psi_{\text{old}}}$ as the old hybrid behavior policy, and the importance ratio is computed as

$$\rho^t(\psi) = \frac{\pi_\psi(\mathbf{a}^t | \mathbf{s}^t)}{\pi_{\psi_{\text{old}}}(\mathbf{a}^t | \mathbf{s}^t)} = \exp(\log \pi_\psi(\mathbf{a}^t | \mathbf{s}^t) - \log \pi_{\psi_{\text{old}}}(\mathbf{a}^t | \mathbf{s}^t)). \quad (29)$$

In LHDPPPO, a learned value-based critic network $V_\phi(\mathbf{s})$ is employed to approximate the expected value of the current state, with parameters ϕ updated from sampled trajectories. Based on this approximation, the Generalized Advantage Estimation (GAE) is constructed as $\hat{A}^t = \sum_{l=0}^{\infty} (\gamma \lambda)^l \delta^{t+l}$, where λ is the GAE parameter, γ is the discount factor, and $\delta^t = r^t + \gamma V_\phi(\mathbf{s}^{t+1}) - V_\phi(\mathbf{s}^t)$ is the Temporal-Difference (TD) residual. This advantage signal can drive the policy update by weighting the likelihood ratio in the PPO clipped surrogate objective, given by [27]

$$\mathcal{L}_{\text{PPO}}(\psi) = -\mathbb{E}^t \left[\min \left(\rho^t(\psi) \hat{A}^t, \text{clip}(\rho^t(\psi), 1 - \kappa, 1 + \kappa) \hat{A}^t \right) \right], \quad (30)$$

where $\kappa \in [0, 1]$ is the clipping parameter. The gradient of this objective is backpropagated through the log-probability of the diffusion policy and ultimately updates the denoising networks $\epsilon_{\psi^c}^c$ and $\epsilon_{\psi^d}^d$. In this manner, LHDPPPO forms another closed training loop for diffusion-based action generation, environment interaction, reward evaluation, and PPO updates are tightly coupled, as shown on the right of Fig. 2.

Meanwhile, the value network is trained using the clipped value loss, calculated by

$$\mathcal{L}_{V_\phi} = \frac{1}{2} \mathbb{E}^t \left[\max \left((V_\phi(\mathbf{s}^t) - \hat{R}^t)^2, (V_{\text{clip}}(\mathbf{s}^t) - \hat{R}^t)^2 \right) \right]. \quad (31)$$

Here, $\hat{R}^t = \hat{A}^t + V_\phi(\mathbf{s}^t)$ is the return target for value learning. $V_{\text{clip}}(\mathbf{s}^t) = V_{\text{old}}(\mathbf{s}^t) + \text{clip}(V_\phi(\mathbf{s}^t) - V_{\text{old}}(\mathbf{s}^t), -\kappa, \kappa)$ is the clipped value prediction used to prevent excessively large value updates, with $V_{\text{old}}(\mathbf{s}^t)$ denoting the value estimate stored when the trajectory was collected.

To prevent premature convergence of the discrete migration policy in the extremely large action space, LHDPPPO introduces an entropy regularization loss for the discrete categorical distributions, calculated by

$$\mathcal{L}_{\text{ent}} = -c_{\text{ent}}^t \left[\frac{1}{M} \sum_{m=1}^M \left(- \sum_{j=1}^{N+1} p_{m,j}^t \log p_{m,j}^t \right) \right]. \quad (32)$$

Here, $p_{m,j}^t = \Pr(e_m^t = j | \mathbf{s}^t)$ denotes the probability assigned by the discrete diffusion policy to migrating the AI agent of AV m to candidate destination edge server j at time slot t , with $j \in \mathbb{N} \cup \{S\}$. c_{ent}^t is an annealed entropy coefficient to ensure stable exploration and efficient convergence during training.

Meanwhile, to stabilize learning of the discrete diffusion actor under the large and multi-dimensional discrete action space, an auxiliary diffusion denoising loss is introduced. The executed migration decisions are converted into a concatenated one-hot vector $\mathbf{x}_0^d \in \{0, 1\}^{M(N+1)}$ and optimized through a diffusion reconstruction objective. This auxiliary loss is applied only to samples with a positive estimated advantage to avoid reinforcing suboptimal behaviors, which is calculated by

$$\mathcal{L}_{\text{diff}} = \mathbb{E} \left[\mathbb{1}(\hat{A}_t > 0) \ell_{\text{diff}}(\mathbf{x}_0^d, \mathbf{s}^t) \right], \quad (33)$$

where $\ell_{\text{diff}}(\mathbf{x}_0^d, \mathbf{s}_t)$ measures the reconstruction error of the discrete diffusion model when denoising the executed migration vector conditioned on the state \mathbf{s}_t , and is instantiated as an L1 reconstruction loss in our implementation.

Eventually, the overall training objective of the proposed LHDPPPO algorithm is given by

$$\mathcal{L} = \mathcal{L}_{\text{PPO}} + c_v \mathcal{L}_{V_\phi} + \mathcal{L}_{\text{ent}} + c_{\text{aux}} \mathcal{L}_{\text{diff}}, \quad (34)$$

where c_v and c_{aux}^t denote the value loss coefficient and the annealed auxiliary diffusion coefficient, respectively.

6 Experimental Results

6.1 Experimental Settings

As illustrated on the left of Fig. 3, we perform simulations on the 6G-enabled vehicular metaverse scenario with real mobility traces of five representative taxis over a 24-hour period, selected from a public taxi dataset containing the

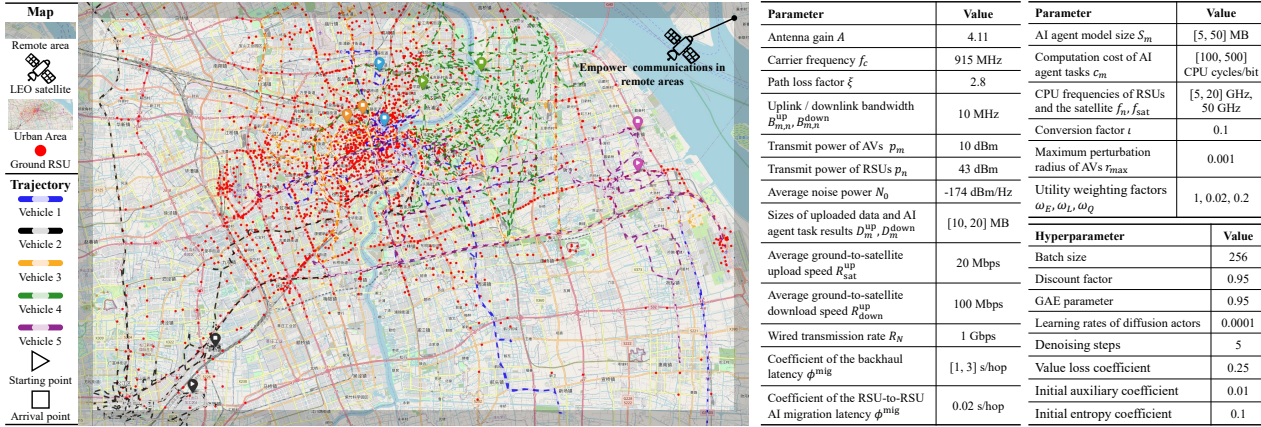


Figure 3 Left: Visualization of the AV trajectories and edge server locations. Right: Parameter and hyperparameter settings in this paper.

trajectories of 4,316 taxis in Shanghai on February 20, 2007 [28]. For the edge server deployment, RSUs are extracted from a real-world dataset comprising approximately 840,000 base stations across China²⁾ and filtered within the target urban region, while a LEO satellite node is incorporated to provide ubiquitous 6G connectivity in remote areas at the boundary of the map. Referring to [9, 11, 29], the environmental parameters and hyperparameters adopted in the experiments are presented on the right of Fig. 3. In addition, the performance of the proposed LHDPPPO algorithm is compared with the following representative baseline methods:

- **Geo-Indistinguishability (Geo-I)** [24]: A non-learning method that perturbs location based on differential privacy, and employs a greedy strategy to select the agent server with the best historical performance.
- **Hybrid PPO (H-PPO)** [30]: A classical hybrid reinforcement learning algorithm in which discrete action selection and continuous parameter optimization are trained in parallel using PPO.
- **GDMs-assisted Hybrid PPO (GHPPPO)** [22]: An extension of H-PPO that introduces a generative diffusion model for discrete action generation while modeling continuous actions using parameterized policies.
- **Hybrid-GDM (HGDM)** [21]: A GDM-based Soft Actor-Critic (SAC) algorithm that expresses both discrete and continuous decisions as continuous latent variables and maps them to executable hybrid actions during inference.
- **PPO-relaxed** [27]: A PPO-based algorithm employing clipped surrogate objectives and GAE for stable policy updates, where discrete migration actions are similarly relaxed into continuous values for tractable training.
- **HDPPPO**: A variant of the proposed LHDPPPO that employs double diffusion chains for hybrid action decisions but removes the LLM-driven reward design loop, in order to evaluate the contribution of reward refinement.

6.2 Numerical Results

Convergence analysis. Fig. 4(a) compares the convergence behaviors of LHDPPPO and representative baselines. Overall, our LHDPPPO achieves a more stable and superior convergence performance. Specifically, several baselines show faster short-term reward gains but then saturate at lower performance levels or suffer from persistent oscillations, indicating difficulty in reliably optimizing the hybrid action mechanism. Moreover, the gap between LHDPPPO and HDPPPO verifies the effectiveness of the LLM-based reward design loop. By refining the reward to better capture the cross-reality privacy-utility coupling, LHDPPPO is guided toward more stable and higher-quality policies. Fig. 4(b) further studies the impact of the learning rate on LHDPPPO. When the learning rate becomes larger (e.g., 10^{-3} or 10^{-2}), the policy updates become more aggressive, resulting in larger variance and making the training more likely to converge to suboptimal solutions. In contrast, an overly small learning rate (e.g., 5×10^{-5}) makes parameter updates overly conservative, which slows down convergence and delays performance improvement. Specifically, compared with a learning rate of 10^{-3} , adopting a moderate learning rate of 10^{-4} improves the final convergence reward by approximately 61.9%, motivating the use of a moderate learning rate (i.e., 10^{-4}) to ensure reliable policy refinement. Fig. 4(c) evaluates the influence of the diffusion denoising steps. Increasing the denoising steps generally improves early-stage learning efficiency, as higher-step diffusion can generate higher-quality hybrid action samples for policy optimization. However, excessively large denoising steps may introduce additional training variance. Quantitatively, compared with 7 denoising steps, the default setting of 5 steps improves the final convergence reward by approximately 58.3%. Therefore, an intermediate denoising-step setting achieves the best tradeoff between convergence stability and final reward.

2) <https://gitcode.com/open-source-toolkit/abc64>

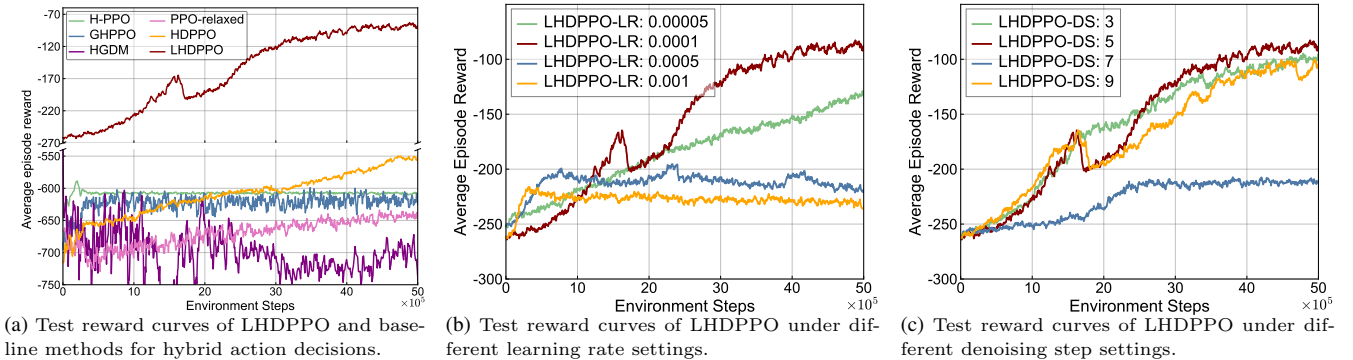


Figure 4 Convergence performance of the proposed LHDPPPO algorithm and the baseline methods. LR: learning rate. DS: denoising step

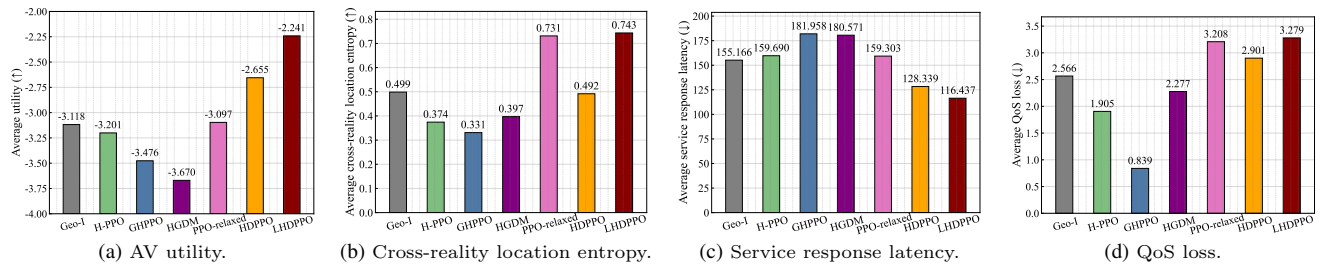


Figure 5 Performance comparison between the proposed LHDPPPO algorithm and the baseline methods.

Performance analysis. Fig. 5 compares the averaged test performance of the proposed LHDPPPO with representative baseline schemes under the cross-reality location privacy protection framework. As shown in Fig. 5(a), HDPPPO, which integrates two diffusion chains without LLM assistance, already achieves strong performance with a high utility, confirming the effectiveness of diffusion-based hybrid action exploration. LHDPPPO further enhances environmental understanding via LLM-driven reward design, leading to the highest AV utility, outperforming the second-best method HDPPPO by 15.6% and the strongest non-diffusion baseline PPO-relaxed by 27.6%. This demonstrates that the proposed LHDPPPO method strikes the most favorable balance between location privacy and user immersion. Fig. 5(b) shows that LHDPPPO attains the highest cross-reality location entropy of 0.743, surpassing the classic privacy-preserving scheme Geo-I by 48.9%, demonstrating its effectiveness in resisting cross-reality inference attacks. Fig. 5(c) shows that LHDPPPO yields the lowest average service response latency, achieving a 9.3% reduction compared with HDPPPO and reductions exceeding 35% relative to most baselines, such as GHPPPO and HGDM, indicating that the privacy improvement does not rely on excessive AI agent migrations that degrade latency. Figure 5(d) illustrates the QoS loss performance of different methods. Although GHPPPO achieves the smallest QoS loss, it performs the worst in terms of privacy protection and latency performance. In contrast, LHDPPPO delivers the strongest privacy protection and the lowest service latency while maintaining an acceptable QoS loss, ensuring both robust location privacy and high-quality immersive experiences for on-board users.

LLM influence analysis. To investigate why LHDPPPO works, Fig. 6 illustrates how cross-reality location entropy varies under the hybrid action mechanism. The surface plot shows that the perturbation radius in the continuous action primarily dominates the entropy variation, while further privacy gains can be achieved by adjusting the included angle α_m^t , which is jointly determined by the perturbation angle in the continuous action and the selected agent server in the discrete migration action. This reveals a strong coupling between the physical perturbed location and the virtual AI agent location: even with a fixed perturbation distance, different relative orientations between the AV and the selected agent server lead to substantially different location privacy levels. The reason is that the difference in direction between the disturbance location and the agent deployment location can simultaneously increase the probabilities of multiple observation points, thereby increasing the uncertainty of the posterior distribution. Through the LLM-driven reward design loop, LHDPPPO identifies α_m^t as a latent but crucial indicator and introduces an additional reward shaping term to encourage a larger discrepancy between the perturbation direction and the server direction, so that the learned policy is guided toward the high-entropy angular peaks rather than only enlarging the perturbation distance.

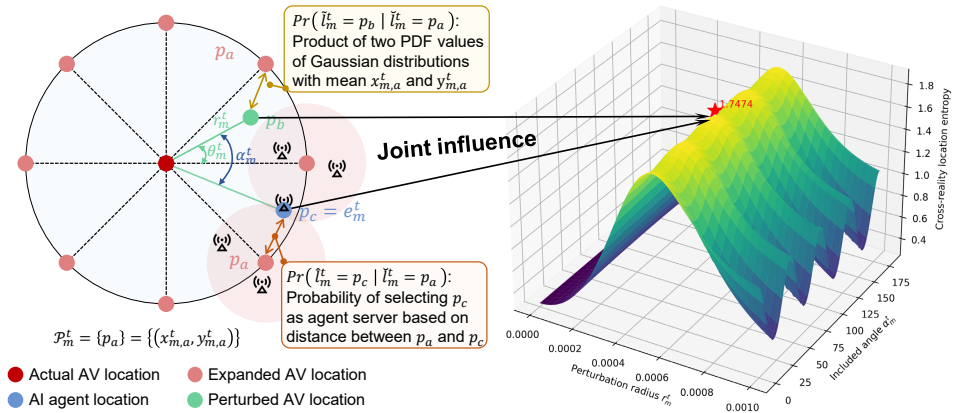


Figure 6 Example of the joint influence of hybrid action mechanisms for cross-reality location privacy protection.

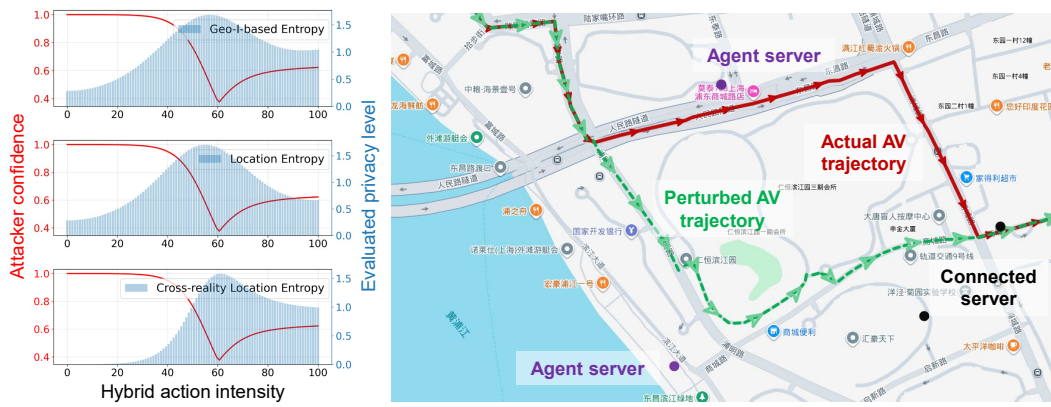


Figure 7 Comparison of the credibility of location privacy metrics under different hybrid action intensities.

Figure 8 Applications of the proposed framework in real scenarios. The figure visualizes the actual and perturbed trajectories of a target AV and its agent server location.

Privacy metric analysis. Fig. 7 compares the evaluated privacy levels with the attacker confidence as the hybrid action intensity increases. We consider two representative baselines about privacy metrics: Geo-I-based entropy for physical location perturbation [24] and location entropy for virtual service migration [11]. A credible privacy metric should show a clear inverse relationship with attacker confidence. However, the Geo-I-based entropy and location entropy fail to satisfy this requirement. When the attacker confidence is high (e.g., action intensity from 0 to 20, confidence close to 1.0), their evaluated privacy levels are not correspondingly low, and their highest privacy values do not coincide with the lowest attacker confidence. This is because both metrics capture only a single dimension of location uncertainty and fail to account for the cross-reality privacy risks jointly induced by AV location disclosure in the physical space and AI agent location exposure in the virtual space. In contrast, the proposed cross-reality location entropy explicitly models this characteristic, yielding privacy evaluations that are consistently aligned with attacker confidence. This property is crucial for reinforcement learning, as it provides a reliable and informative reward signal for stable and effective policy optimization.

Case study in real scenarios. Fig. 8 presents a real-map example to illustrate how the proposed framework performs cross-reality location privacy protection in practice. The red polyline denotes the actual AV trajectory, while the green polyline shows the perturbed trajectory generated by the learned privacy policy. We can observe that the policy produces reasonable perturbations along the route, so that the released locations deviate from the true path while avoiding excessive QoS degradation. Moreover, the framework jointly controls the virtual-space decision by dynamically selecting agent servers at different time instants. As shown in Fig. 8, the selected agent servers are distributed around the neighborhoods of both the actual and perturbed trajectories, rather than being fixed to a single closest server. This coupled strategy maximally confuses the attacker by preventing a consistent cross-reality alignment between the reported physical trajectory and the observed AI agent deployment, thereby reducing attacker confidence in tracing the true route. The real-world experiments indicate that the proposed cross-reality location privacy protection framework maintains privacy protection and user immersion across dynamic vehicular environments, demonstrating a certain degree of generalizability.

7 Conclusion

This paper has proposed a cross-reality location privacy protection framework to mitigate cross-reality location privacy leakage for agentic AI-driven AVs in 6G-enabled vehicular metaverses. By adopting a hybrid action mechanism that jointly employs continuous location perturbation in reality and discrete privacy-aware AI agent migration in virtuality, the proposed framework achieves unified cross-reality location privacy preservation while maintaining user immersion. A cross-reality location entropy metric has been designed to quantify the uncertainty of AV positions under hybrid actions and to support real-time privacy assessment. Combining location privacy, service latency, and QoS loss, a non-convex mixed-integer programming problem has been established for optimizing the hybrid action mechanism. To address the formulated problem, we have developed an LLM-enhanced Hybrid Diffusion Proximal Policy Optimization (LHDPPPO) algorithm, which combines LLM-driven informative reward design with double GDMs-based policy exploration and PPO-based stable policy updates to improve learning performance and scalability. Extensive experiments on real-world mobility and base station datasets have demonstrated that the proposed framework effectively protects location privacy while ensuring immersion for on-board users, indicating its practical applicability for large-scale 6G-enabled vehicular metaverse deployments. Future work will explore how heterogeneous AV mobility patterns, from correlated commuting routes to random delivery trajectories, affect the privacy-immersion trade-off and how adaptive mechanisms can provide more balanced privacy protection.

References

- 1 Xie G, Xiong Z, Zhang X et al. Towards the vehicular metaverse: Exploring distributed inference with transformer-based diffusion model, *IEEE Trans Veh Technol*, 2024, 73(12): 19931–19936.
- 2 Chen J, Kang J, Xu M et al. Efficient twin migration in vehicular metaverses: Multi-agent split deep reinforcement learning with spatio-temporal trajectory generation, *IEEE Trans Mobile Comput*, 2025.
- 3 Kang J, Tong Y, Zhong Y et al. Diffusion-based auction mechanism for efficient resource management in 6G-enabled vehicular metaverses, *Sci China Inf Sci*, 2025, 68: 1–16.
- 4 Seid A M, Abishu H N, Hevesli M et al. A multi-agent DRL-based dynamic resource allocation in O-RAN-enabled TN-NTN metaverse services, *IEEE Trans Commun*, 2025, 73(12): 14243–14259.
- 5 Kang J, Luo X, Nie J et al. Blockchain-based pseudonym management for vehicle twin migrations in vehicular edge metaverse, *IEEE Internet Things J*, 2024.
- 6 Yu J. Agentic vehicles for human-centered mobility, *arXiv preprint arXiv:2507.04996*, 2025.
- 7 Auda J, Gruenfeld U, Faltaous S et al. A scoping survey on cross-reality systems, *ACM Comput Surv*, 2023, 56: 1–38.
- 8 Hiroi Y, Hatada Y, Hiraki T. Cross-reality lifestyle: Integrating physical and virtual lives through multi-platform metaverse, *arXiv preprint arXiv:2504.21337*, 2025.
- 9 Luo X, He J, Fu Y et al. Incentivizing pseudonym exchange with trajectory prediction for privacy-enhanced vehicular metaverses: A diffusion-based auction approach, *IEEE Trans Mobile Comput*, 2025.
- 10 Min M, Zhu H, Ding J et al. Personalized 3D location privacy protection with differential and distortion geo-perturbation, *IEEE Trans Depend Secure Comput*, 2023, 21: 3629–3643.
- 11 Wang W, Zhou X, Qiu T et al. Location-privacy-aware service migration against inference attacks in multiuser MEC systems, *IEEE Internet Things J*, 2023, 11: 1413–1426.
- 12 Luo X, Wen J, Kang J et al. Privacy attacks and defenses for digital twin migrations in vehicular metaverses, *IEEE Netw*, 2023, 37: 82–91.
- 13 Ullah I, Ali Shah M, Khan A et al. Location privacy schemes in vehicular networks: taxonomy, comparative analysis, design challenges, and future opportunities, *ACM Comput Surv*, 2025, 57: 1–44.
- 14 Liu B, Zhou W, Zhu T et al. Location privacy and its applications: A systematic study, *IEEE Access*, 2018, 6: 17606–17624.
- 15 Liu Y, Zhang Y, Su S et al. BlockSC: A blockchain empowered spatial crowdsourcing service in metaverse while preserving user location privacy, *IEEE J Sel Areas Commun*, 2023, 42: 880–892.
- 16 Wang L, Pang S, Gui H et al. Sustainable energy-efficient multi-objective task processing based on edge computing, *IEEE Trans Netw Serv Manag*, 2025, 22(4): 3092–3105.
- 17 Emara K. Safety-aware location privacy in VANET: Evaluation and comparison, *IEEE Trans Veh Technol*, 2017, 66: 10718–10731.
- 18 Li M, Chen Y, Kumar N et al. Quantifying location privacy for navigation services in sustainable vehicular networks, *IEEE Trans Green Commun Netw*, 2022, 6: 1267–1275.
- 19 Du H, Zhang R, Liu Y et al. Enhancing deep reinforcement learning: A tutorial on generative diffusion models in network optimization, *IEEE Commun Surv Tutor*, 2024, 26: 2611–2646.
- 20 Ning P, Wang H, Tang T et al. Diffusion-based deep reinforcement learning for resource management in connected construction equipment networks: A hierarchical framework, *IEEE Trans Wireless Commun*, 2025.
- 21 Kang Y, Wen J, Kang J et al. Hybrid-generative diffusion models for attack-oriented twin migration in vehicular metaverses, *IEEE Trans Veh Technol*, 2025.
- 22 Wang K, Wang X, Zhao N et al. Uplink RSMA in LEO satellite communications: A perspective from generative artificial intelligence, *IEEE Trans Veh Technol*, 2025.
- 23 Sheng M, Zhou D, Bai W et al. Coverage enhancement for 6G satellite-terrestrial integrated networks: performance metrics, constellation configuration and resource allocation, *Sci China Inf Sci*, 2023, 66: 130303.
- 24 Andrés M E, Bordenabe N E, Chatzikokolakis K et al. Geo-indistinguishability: Differential privacy for location-based systems, In: *Proc ACM SIGSAC Conf Comput Commun Secur*, 2013, 901–914.
- 25 Rényi A. On measures of entropy and information, In: *Proc Fourth Berkeley Symp Math Stat Probab*, Vol. 1: Contributions to the Theory of Statistics, Univ California Press, 1961, 547–562.
- 26 Cao Y, Zhao H, Cheng Y et al. Survey on large language model-enhanced reinforcement learning: Concept, taxonomy, and methods, *IEEE Trans Neural Netw Learn Syst*, 2025, 36: 9737–9757.
- 27 Zhang R, Zhao C, Du H et al. Embodied AI-enhanced vehicular networks: An integrated vision language models and reinforcement learning method, *IEEE Trans Mobile Comput*, 2025, 24(11): 11494–11510.
- 28 Zhu H, Li M, Fu L et al. Impact of traffic influxes: revealing exponential intercontact time in urban VANETs, *IEEE Trans Parallel Distrib Syst*, 2010, 22: 1258–1266.
- 29 Chen Z, Yi W, Nallanathan A et al. Distributed digital twin migration in multi-tier computing systems, *IEEE J Sel Top Signal Process*, 2024, 18: 109–123.
- 30 Fan Z, Su R, Zhang W et al. Hybrid actor-critic reinforcement learning in parameterized action space, In: *Proc Int Joint Conf Artif Intell (IJCAI)*, Macao, China, 2019, 2279–2285.